Finite element modeling and validation of guided wave scattering

P. Fromme

P. Fromme, "Finite element modeling and validation of guided wave scattering," Proc. SPIE 10972, Health Monitoring of Structural and Biological Systems XIII, 1097225 (1 April 2019); doi: 10.1117/12.2513673

SPIE.

Event: SPIE Smart Structures + Nondestructive Evaluation, 2019, Denver, Colorado, United States

Finite Element Modelling and Validation of Guided Wave Scattering

P. Fromme
Department of Mechanical Engineering, University College London, WC1E 7JE, UK

ABSTRACT

Numerical simulations such as Finite Element (FE) modelling allow the simulation and prediction of guided wave propagation and scattering. Specific considerations concerning the choice of mesh, element type, time step, and analysis method are required to ensure stable and accurate simulations. Modeling considerations and validation against experimental results are shown for two examples of increasing complexity. The approximation of complex geometries and the effects on guided wave propagation are discussed. Examples concerning guided wave scattering at defects in single and multiple metallic layers of plate structures were compared against experimental results.

Keywords: Lamb Waves, Scattering, Finite Element Analysis

1. INTRODUCTION

Guided ultrasonic waves allow the efficient monitoring of large structures [1], as long propagation distances can be achieved, especially at low excitation frequencies [2]. This has been employed for the nondestructive monitoring of different types of structures and defects, e.g. pipes [3], plates [4], bonded stiffeners [5], multi-layered structures [6], and composites [7]. Localized and distributed array systems using low-frequency guided waves have been developed for the detection and localization of defects in plate structures [8-10]. The sensitivity for crack-like defects can be improved by advanced signal processing, e.g., minimum variance imaging taking the scattering directionality pattern around the crack into account [11].

Fatigue crack growth in multi-layered metallic components constitutes a significant maintenance problem for ageing aircraft structures [12]. High frequency guided waves have been employed to monitor fatigue crack growth at fastener holes [13, 14] and to detect defects in multi-layered metallic structures [15]. For the aerospace industry, composite structures offer improved strength to weight ratio, but are subject to barely visible impact damage [16]. The propagation of guided ultrasonic waves depends on the material anisotropy, requiring good understanding for experimental design and analysis [17, 18]. Guided ultrasonic waves have been successfully employed to detect delaminations and impact damage in composite structures [19-21].

The scattering of the A_0 Lamb wave mode at circular holes has been modelled analytically and numerically, verified experimentally [22-24]. The scattering of guided waves at fatigue cracks emanating from a fastener hole has been simulated and compared to experimental measurements for single metallic layers [25-27] and multi-layered structures [28]. The scattering pattern of the A_0 Lamb wave mode at notches in a plate has been investigated from Finite Element (FE) simulations for a range of geometrical parameters, e.g., defect orientation, length, and depth, and measured experimentally [29].

In this contribution, for two problems of increasing complexity ranging from a notch in an metallic plate to fatigue cracks in multi-layered structures, the considerations for numerical modelling of the guided ultrasonic wave propagation and scattering are discussed. Comparison to experimental results for allows for the validation of the numerical models and better understanding of the underlying physics.

Health Monitoring of Structural and Biological Systems XIII, edited by Paul Fromme, Zhongqing Su, Proc. of SPIE Vol. 10972, 1097225 · © 2019 SPIE
CCC code: 0277-786X/19/$18 · doi: 10.1117/12.2513673

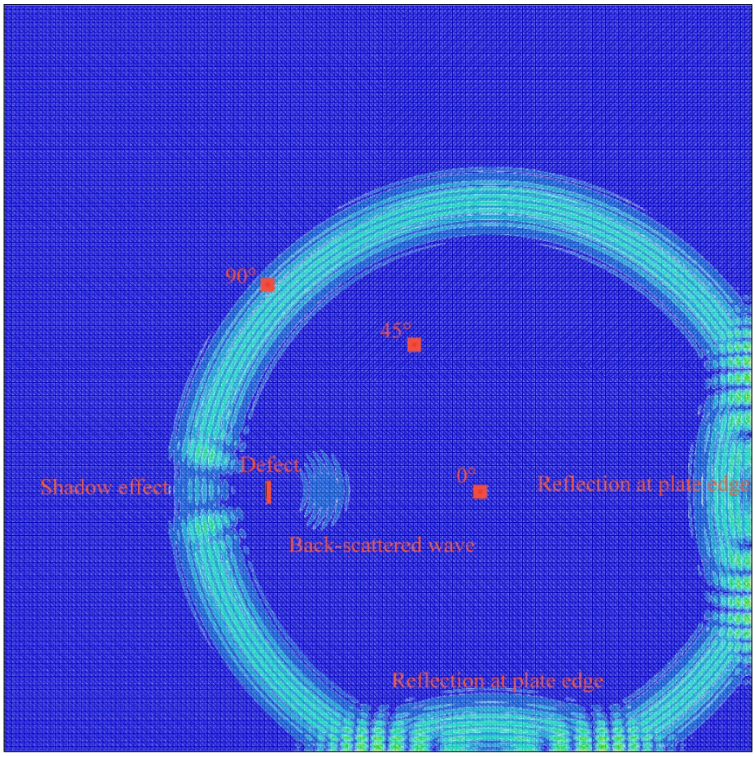

Fig. 1. Time snapshot of FE simulation for aluminum plate with notch; A_0 mode, f = 100 kHz; λ = 19 mm; a = 20 mm; wave propagating radially outwards from excitation point, back-scattered wave at notch and edge reflections visible.

2. SCATTERING AT A NOTCH IN ALUMINIUM PLATE

The scattering of the fundamental anti-symmetric A_0 Lamb wave mode at notches in large aluminum plates (Fig. 1) was simulated using three-dimensional (3D) Finite Element (FE) models. The influence of incident wave direction to the notch orientation, notch length and depth was investigated [29]. The complete 1 m x 1 m x 5 mm thick aluminum plate (Fig. 1) was modelled using linear brick elements in ABAQUS Explicit. Notches of varying length and depth were modelled by removing the required elements to match the experimental setup, as described in [29]. No mesh refinement around the defect was implemented and a straight-forward Cartesian mesh was employed. This allows good control over the element size and measurement grid to compare simulations with and without a defect and to interpolate the data to exactly match the experimental measurement grid. However, without mesh refinement the linear elements potentially do not correctly approximate the stress concentration at the defect, especially the defect tips. Especially for cracks this might lead to an under-estimation of the scattering contribution from the crack tips. For the scenario investigated here, the notch length was comparable to the wavelength of the incident A_0 Lamb wave mode and the scattering along the length of the defect was assumed to contribute significantly to the observed scattered wavefield.

The element size and time step were chosen to adhere to the usual stability criteria, and explicit time integration was used. Different angles of the incident wave relative to the defect orientation were implemented by choosing an excitation point 300 mm from the defect center at the required angle. The excited wave propagates radially outwards from the excitation point. The distance was chosen large enough that at the defect location the curvature (radius) of the incident wave front can be neglected and it can be considered as a plane incident wave when compared to the largest considered defect length (here: 20 mm). A narrowband 5 cycle toneburst with a center frequency of 100 kHz was chosen as the excitation pulse, corresponding to a wavelength λ for the A_0 mode of 19 mm.

On points in a square area around the defect, the out-of-plane displacement at the center (mid-plane) node was recorded to capture selectively the A_0 Lamb wave mode. Below the cut-off frequency of the higher Lamb wave modes, the A_0, S_0, and SH_0 modes can exist, but only the A_0 mode has an out-of-plane component at the center plane. The recorded time trace at each monitoring node was saved and time gated to remove edge reflections from the plate.

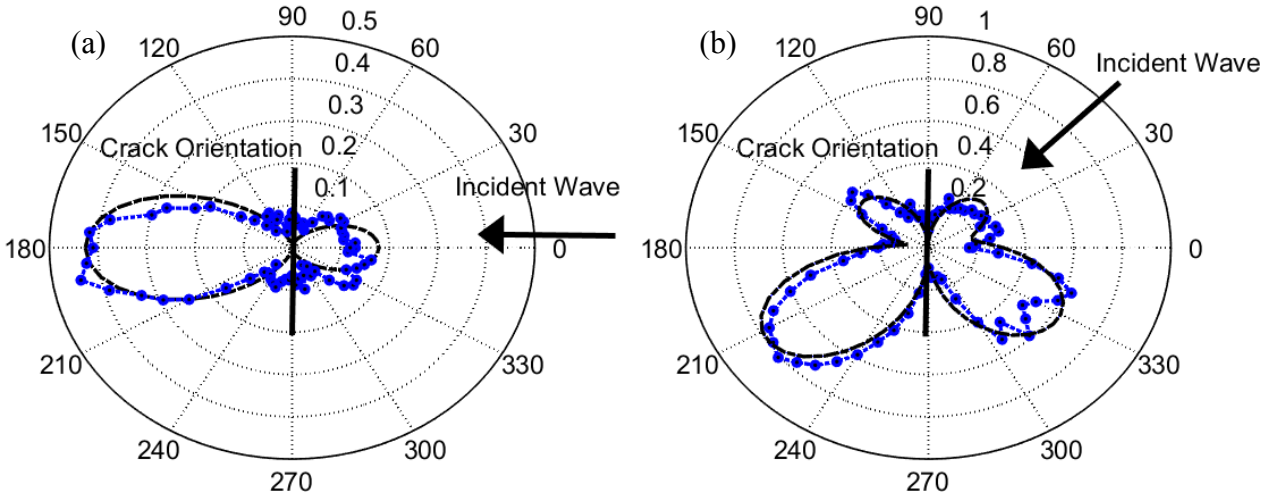

Fig. 2. Normalized amplitude (polar plot monitored at 30 mm radius) of A_0 Lamb wave mode scattered at notch; f = 100 kHz; wavelength λ = 19 mm; notch length a = 20 mm; experiment notch (blue, dotted), FE simulation (black, dash-dotted): a) ½ thickness, 0° incident wave; b) through thickness, 90° incident wave.

Using Fast Fourier Transform (FFT) the complex magnitude (amplitude and phase) at the center frequency was extracted for each monitoring node. For the models with the defect, this captures the combined incident and scattered wave field. Further FE simulations were run with the same excitation locations, but without any defect to record only the incident wave field. The amplitude of the scattered wave at the notch was calculated by taking the difference between the complex magnitudes for each point with and without a defect. The scattered wave amplitude on a circle with radius 30 mm and angular step of 5 degree was obtained by interpolating bi-linearly between the regularly spaced monitoring nodes. The methodology is described in detail in a previous contribution [29].

The FE simulation results were compared to experimental measurements, matching as much as possible the geometries and evaluation methods, as described in [29]. An initial measurement was done for each excitation transducer before the notch was milled to record the incident wave field, and then for each notch depth. Due to the re-positioning of the plate after each milling step, when the difference between the complex magnitudes was calculated, the repeatability was limited to a noise level of about 5% of the amplitude of the incident wave.

Polar plots of the amplitude patterns (normalized to incident wave amplitude) from experiments and FE simulations are shown in Fig. 2 for two cases. Fig. 2a shows the scattered wave pattern for the incident wave perpendicular to a 20 mm long notch halfway through the plate thickness. The predicted scattering pattern is symmetric, with a small back-scattered lobe in the 0° direction and a larger shadow area in the 180° direction, where the defect blocks part of the incident wave path and reflects some of the energy. For the lobe around the 180° direction a good agreement between FE simulation and experiments can be observed, with a slight asymmetry of the measurement results. For the back-scattered wave around the 0° direction, the amplitudes approximately match, but the pattern of the experimental results is not that clear as the amplitude is only about three times the noise level due to the re-positioning of the plate after milling. The mode conversion to the S_0 mode at the part-thickness defect was not evaluated but could be investigated from the FE simulations. Fig. 2b shows the scattering at a through-thickness notch for an incident wave direction of 45°. Due to the larger defect depth, the overall scattered wave amplitude is higher than observed in Fig. 2a. A distinct pattern with two larger and two smaller lobes can be observed and matches well between measurements and FE simulations [29]. Good agreement of the measured and simulated amplitude patterns was found, and the FE simulations validated. Distinct angular patterns of the scattered guided wave were observed, which can be considered for the prediction of defect detection sensitivity using distributed guided wave arrays, e.g. minimum variance imaging [11].

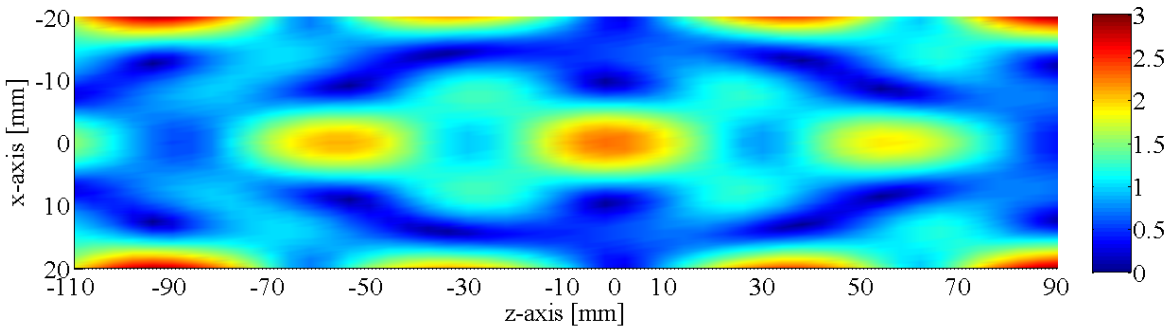

Fig. 3: FE simulation of amplitude variation along multi-layered tensile specimen (width 40 mm) for 3 excitation point forces (z = -110 mm) to match experimental configuration, excitation frequency: 115 kHz.

3. WAVE PROPAGATION AND SCATTERING AT FATIGUE CRACK IN A MULTI-LAYERED SPECIMEN

As a more complex geometry, the wave propagation and scattering of low frequency guided wave modes in a multi-layered specimen were investigated [28]. The multi-layered structure consists of two aluminum layers (each 3 mm thickness) with a 0.2 mm thick sealant layer. Experimentally the growth of a fatigue crack in the bottom (hidden) layer of the multi-layered structure at a fastener hole was investigated. The scattered guided wave field around the fastener hole was measured before crack initiation and for a macroscopic crack in the bottom layer approximately 5 mm long. The tensile specimens employed had a limited width of 40 mm to fit into the test machine grips and multi-modal guided wave propagation with different mode shapes across the specimen width was observed. Even considering only flexural modes (similar thickness mode shape to A_0 Lamb wave mode), at the chosen excitation frequency of 115 kHz three propagating wave modes existed.

Using a 3D model in ABAQUS/Explicit, FE simulations were conducted to investigate the wave propagation and scattering in the tensile specimen [28]. The specimen geometry was again modelled using a Cartesian mesh with linear brick elements (C3D8R) with an element size for the plates of 0.5 mm x 0.5 mm x 0.75 mm, and for the sealant of 0.5 mm x 0.5 mm x 0.1 mm. The in-plane element size was much smaller than required by the usual stability criteria compared to the wavelength, but were chosen to achieve acceptable ratios to the required small element size in the thickness direction. Each of the 3 mm thick aluminum adherents was modelled with 4 linear elements through the thickness to accurately catch the flexural mode shape. The thin sealant layer was modelled with 2 elements through the thickness to approximate the rather large shearing predicted from the mode shapes. Figure 3 shows the distinctive interference pattern between the three flexural wave modes as they propagate along the multi-layered specimen. Reasonably good agreement with experimental measurements was found [28].

The scattering at the fastener hole and fatigue crack was simulated using the FE model. The hole (radius 3 mm) was approximated by the Cartesian mesh, removing the required elements. This approximated the circular hole shape with a stepped structure with 0.5 mm steps from the size of the brick elements and might introduce some error for the scattered field. From a comparison of the FE simulation predictions to the measurement for the undamaged hole, a good agreement was found except for a slight asymmetry of the experimental results, potentially due to an asymmetry of the incident wave field [28]. The approximately 4.8 mm long fatigue crack in the bottom aluminum layer was modelled as a zero-width crack of 5 mm length through the thickness of the bottom layer (3 mm) by having the corresponding elements along the crack surface not connected. This does not allow for potential contact between the crack surfaces, but as the crack could be well observed using an optical microscope, the modelling as an open crack was not considered to introduce a significant error.

Figure 4 shows the comparison between the FE simulations (Fig. 4a) and the experimental results (Fig. 4b). The incident wave propagates from bottom to top and at the hole a high amplitude consistent with the reflection at a free surface can be observed for both cases. As the fastener hole diameter is small compared to the incident mode wavelengths, a high amplitude behind the hole (top) can also be seen. In front of the hole (bottom), a semi-circular area of high amplitude due to the constructive interference of the incident and scattered waves can be seen. For both numerical and experimental an asymmetry due to the hidden crack at the right-hand side of the hole (in bottom aluminum layer) can be observed. Directly in front of the crack, a higher amplitude at the hole can be seen and the scattering pattern is twisted away from

the defect. Overall, the influence of the hidden fatigue crack on the guided wave scattering could be well predicted from the FE simulations.

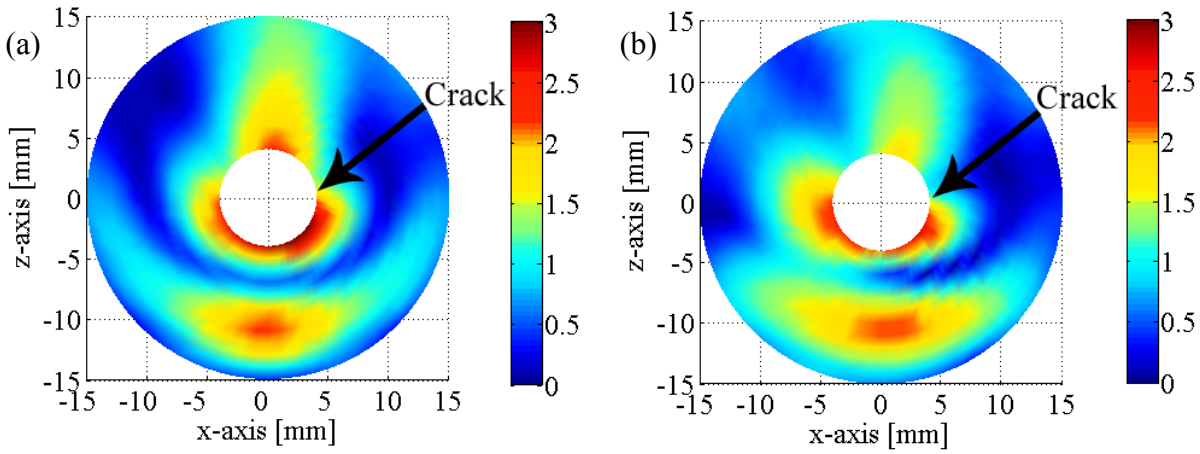

Fig. 4: Comparison of scattered field wave around hole (r = 3 mm) between a) FE simulation and b) measurement for approximately 5 mm long defect in bottom layer (indicated by arrow); amplitude at center frequency 115 kHz from FFT, incident wave propagating from bottom to top.

4. CONCLUSIONS

The scattering of guided ultrasonic waves at defects in metallic structures were predicted from FE simulations and compared with experimental results for validation. For the case of part-through and through thickness notches in an aluminum plate good agreement between the scattered field directivity patterns was obtained, with some limitation of the experimental results due to the required re-positioning of the plate after each milling step. Employing a Cartesian grid without mesh refinement around the defect was found to accurately model the scattering behavior at a large defect comparable in size to the A_0 Lamb wave mode wavelength. For the case of a fatigue crack at a fastener hole in a multi-layered structure care had to be taken with the element size through the thickness to accurately model the mode shapes, resulting in a small element size compared to the wavelength. This was then found to be sufficient to approximate the circular fastener hole and crack with the Cartesian mesh and to accurately predict the change in the scattered wave field due to fatigue crack growth. For anisotropic materials additional considerations are required to accurately capture the guided wave propagation and scattering, e.g. for impact damage and delaminations in composite plates.

REFERENCES

[1] Rose, J.L., “Standing on the shoulders of giants: An example of guided wave inspection,” Mat. Eval. 60, 53-59 (2002).

[2] Dalton, R.P., Cawley, P. and Lowe, M.J.S, "The potential of guided waves for monitoring large areas of metallic aircraft fuselage structure." J. Nondestruct. Eval. 20, 29-46 (2001).

[3] Howard, R. and Cegla, F. "Detectability of corrosion damage with circumferential guided waves in reflection and transmission." NDT&E Int. 91, 108-119 (2017).

[4] Croxford, A.J., Wilcox, P.D., Drinkwater, B.W. and Konstantinidis, G., “Strategies for guided-wave structural health monitoring,” Proc. Roy. Soc. A 463, 2961-2981 (2007).

[5] Fan, Z., Castaings, M., Lowe, M.J.S., Biateau, C. and Fromme, P., “Feature-guided waves for monitoring adhesive shear modulus in bonded stiffeners,” NDT&E Int. 54, 96-102 (2013).

[6] Fromme, P., Reymondin, J.-P., and Masserey, B., “High frequency guided waves for disbond detection in multi-layered structures,” Acta Acust. united Ac. 103, 932-940 (2017).

[7] Endrizzi, M., Murat, B.I.S., Fromme, P. and Olivo, A., “Edge-illumination X-ray dark-field imaging for visualising defects in composite structures,” Compos. Struct. 134, 895-899 (2015).

[8] Fromme, P., Wilcox, P.D., Lowe, M.J.S. and Cawley, P., “On the development and testing of a guided ultrasonic wave array for structural integrity monitoring,” IEEE Trans. Ultrason. Ferroelectr. Freq. Control 53, 777-785 (2006).

[9] Michaels, J.E. and Michaels, T.E., "Guided wave signal processing and image fusion for in situ damage localization in plates," Wave Motion 44, 482-492 (2007).
[10] Fromme, P., "Health Monitoring of Plate Structures Using Guided Waves," Proc. of SPIE 6935, W9350 (2008).
[11] Hall, J.S., Fromme, P. and Michaels, J.E., "Guided Wave Damage Characterization via Minimum Variance Imaging with a Distributed Array of Ultrasonic Sensors," J. Nondestruct. Eval. 33, 299-308 (2014).
[12] Masserey, B. and Fromme, P., "Fatigue Crack Growth Monitoring using High Frequency Guided Waves," Struct. Health Monit. 12, 484-493 (2013).
[13] Masserey, B. and Fromme, P., "In-Situ Monitoring of Fatigue Crack Growth using High Frequency Guided Waves," NDT&E Int. 71, 1-7 (2015).
[14] Chan, H., Masserey B. and Fromme, P., "High frequency guided ultrasonic waves for hidden fatigue crack growth monitoring in multi-layer model aerospace structures," Smart Mater. Struct. 24, 025037 (2015).
[15] Masserey, B., Raemy, C. and Fromme, P., "High-frequency guided ultrasonic waves for hidden defect detection in multi-layered aircraft structures," Ultrasonics 54, 1720-1728 (2014).
[16] Swait, T. J., Jones, F. R. and Hayes, S. A., "A practical structural health monitoring system for carbon fibre reinforced composite based on electrical resistance," Compos. Sci. Technol. 72, 1515-1523 (2012).
[17] Castaings, M. and Hosten, B., "Guided waves propagating in sandwich structures made of anisotropic, viscoelastic, composite materials," J. Acoust. Soc. Am. 113, 2622-2634 (2003).
[18] Fromme, P., Pizzolato, M., Robyr, J.-L. and Masserey, B., "Lamb wave propagation in monocrystalline silicon wafers," J. Acoust. Soc. Am. 143, 287-295 (2018).
[19] Toyama, N. and Takatsubo, J., "Lamb wave method for quick inspection of impact-induced delamination in composite laminates," Compos. Sci. Technol. 64, 1293-1300 (2003).
[20] Tan, K.S., Guo, N., Wong, B.S. and Tui, C.G., "Experimental evaluation of delaminations in composite plates by the use of Lamb waves," Compos. Sci. Technol. 53, 77-84 (1995).
[21] Murat, B.I.S., Khalili, P. and Fromme, P., "Scattering of guided waves at delaminations in composite plates," J. Acoust. Soc. Am. 139, 3044-3052 (2016).
[22] Pao, Y.H. and Chao, C.C., "Diffractions of flexural waves by a cavity in an elastic plate," AIAA J. 2, 2004-2010 (1964).
[23] Fromme, P. and Sayir, M.B., "Measurement of the scattering of a Lamb wave by a through hole in a plate," J. Acoust. Soc. Am. 111, 1165-1170 (2002).
[24] Diligent, O., Grahn, T., Bostrom, A., Cawley, P. and Lowe, M.J.S., "The low-frequency reflection and scattering of the S0 Lamb wave mode from a circular through-thickness hole in a plate: Finite Element, analytical and experimental studies," J. Acoust. Soc. Am. 112, 2589-2601 (2002).
[25] Fromme, P. and Sayir, M.B., "Detection of cracks at rivet holes using guided waves," Ultrasonics 40, 199-203 (2002).
[26] Liu, H., Chen, X., Michaels, J.E., Michaels, T.E. and He, C., "Incremental scattering of the A0 Lamb wave mode from a notch emanating from a through-hole," Ultrasonics 91, 220-230 (2019).
[27] Masserey, B. and Fromme, P., "Analysis of high frequency guided wave scattering at a fastener hole with a view to fatigue crack detection," Ultrasonics 76, 78-86 (2017).
[28] Kostson, E. and Fromme, P., "Fatigue crack growth monitoring in multi-layered structures using guided ultrasonic waves," J. Phys.: Conf. Ser. 195, 012003 (2009).
[29] Rouge, C. and Fromme, P., "Directivity of guided ultrasonic wave scattering at notches and cracks," J. Phys.: Conf. Ser. 269, 012018 (2011).